NATIONAL AERONAUTICS AND SPACE ADMINISTRATION

Technical Report No. 32-1007

Trajectory Design for Impulsive Earth–Mars–Earth Trajectories Launched in 1969 and 1971

Peter H. Feitis

GPO PRICE $ _____

CFSTI PRICE(S) $ _____

Hard copy (HC) 2.00

Microfiche (MF) .50

ff 653 July 65

FACILITY FORM 602

N67 13195 (ACCESSION NUMBER)

29 (PAGES)

CR-80520 (NASA CR OR TMX OR AD NUMBER)

(THRU)

1 (CODE)

30 (CATEGORY)

JET PROPULSION LABORATORY
CALIFORNIA INSTITUTE OF TECHNOLOGY
PASADENA, CALIFORNIA

December 1, 1966

NATIONAL AERONAUTICS AND SPACE ADMINISTRATION

Technical Report No. 32-1007

Trajectory Design for Impulsive Earth – Mars – Earth Trajectories Launched in 1969 and 1971

Peter H. Feitis

Approved by:

T. W. Hamilton, *Manager*
Systems Analysis Section

JET PROPULSION LABORATORY
CALIFORNIA INSTITUTE OF TECHNOLOGY
PASADENA, CALIFORNIA

December 1, 1966

Copyright © 1966
Jet Propulsion Laboratory
California Institute of Technology

Prepared Under Contract No. NAS 7-100
National Aeronautics & Space Administration

CONTENTS

I. Introduction 1

II. Mathematical Model 1

III. Presentation of Trajectory Data 4

IV. Computer Program Description 4

V. Discussion of Contour Plots 6

VI. 1971 Opportunity 6

VII. Communication Advantage of an Earth–Mars–Earth Mission 20

VIII. Flyby Geometry 23

Nomenclature 23

References 24

TABLE

1. Flyby altitude and required ΔV for three types of maneuvers 3

FIGURES

1. Lighting conditions for Mars flyby 1

2. Mars encounter geometry 2

3. *DVL* contours. Earth–Mars–Earth 1968–1969 5

4. *DVP* contours. Earth–Mars–Earth 1968–1969 7

5. *DVT* contours. Earth–Mars–Earth 1968–1969 8

6. *HP* contours. Earth–Mars–Earth 1968–1969 9

7. *ZAPA* contours. Earth–Mars–Earth 1968–1969 10

8. *ZALD* contours. Earth–Mars–Earth 1968–1969 11

FIGURES (Cont'd)

9. *T* contours. Earth–Mars–Earth 1968–1969 12
10. *DVL* contours. Earth–Mars–Earth 1970–1971 13
11. *DVP* contours. Earth–Mars–Earth 1970–1971 14
12. *DVT* contours. Earth–Mars–Earth 1970–1971 15
13. *HP* contours. Earth–Mars–Earth 1970–1971 16
14. *ZAPA* contours. Earth–Mars–Earth 1970–1971 17
15. *ZALD* contours. Earth–Mars–Earth 1970–1971 18
16. *T* contours. Earth–Mars–Earth 1970–1971 19
17. Ecliptic view of 1971 Earth–Mars–Earth trajectory 21
18. Time, days from Mars departure 22

ABSTRACT

This Report discusses the trajectory design for a spacecraft which returns to the vicinity of the Earth after the Mars encounter. It is possible to fly a purely ballistic roundtrip mission with relatively short flight time. A wide variety of encounter geometries at Mars is possible, some of which are suitable for television pictures and other scientific experiments. If it is necessary to carry out a velocity correction maneuver at Mars due to the difference in asymptote of approach and departure, the roundtrip trajectory is called "impulsive." By using a velocity increment, it is often possible to improve the trajectory characteristics or mission payload.

The Report also describes the method and associated computer programs used to analyze Earth–Mars–Earth trajectories based on the patched conic model. The return probe can transmit up to 1000 times more data during the Earth-encounter phase than the non-return flyby probe such as the JPL *Mariner IV*.

Due to the large communication distances and small transmitter powers involved, the Mars flyby spacecraft can return severely limited quantities of data. The Mars orbiter can obtain a great deal more data and has been the topic of much investigation.

It has been concluded that the 1971 Earth-to-Mars launch period is most advantageous for Earth-return missions, compared to the 1969, 1973 and 1975 Mars opportunities.

AUTHOR

I. INTRODUCTION

It was the purpose of this Report[1] to design working charts showing characteristics of Earth–Mars–Earth trajectories which would enable the user to make some of the important tradeoffs. The intent was to generate working graphs similar to those used for the actual design of interplanetary missions such as *Mariner II* to Venus and *Mariner IV* to Mars (Ref. 1), and also presently being used to design one-way missions to Jupiter and Mercury. Such data consist of contour plots of various trajectory parameters plotted as a function of launch date from Earth and arrival date at Mars.

[1]This Report was presented as a technical paper to the American Astronautical Society at the Space Flight Mechanics Specialist Conference held at the University of Denver, Denver, Colorado, July 6–8, 1966.

A very extensive summary (Ref. 2) was delivered on the most important work in the design of trajectory analysis for one-way and multiple planet-trajectory missions.

The first attempt to generate trajectory design plots for ballistic round-trip missions to Mars and Venus (Ref. 3) was probably made by Stanley E. Ross. The data are presented in the form of contour charts which show loci of constant launch energy, periplanet distance, and hyperbolic excess speed at Mars in the Earth launch date–Mars arrival date plane. The present Report can be regarded as an extension of the data for the 1969 and 1971 Mars opportunities to the case of impulsive Earth–Mars–Earth trajectories.

II. MATHEMATICAL MODEL

The Earth–Mars–Earth trajectory will be assumed to consist of three patched conics: the heliocentric Earth–Mars leg, the Mars-centered conic trajectory, and the heliocentric Mars–Earth leg. The launch date at Earth, arrival date at Mars, and arrival date at Earth are denoted by TL, TA, TA', respectively. The total trip time is designated by T [2].

Given TL and TA, the Earth-to-Mars conic trajectory is readily computed, and results in the following trajectory parameters:

DVL – the ΔV at launch beginning in Earth parking orbit[3].

DLA – the declination of the outgoing asymptote at the Earth.

VHP – the asymptotic speed at Mars upon arrival.

$ZAPA$ – the angle between the incoming asymptote at Mars and the Sun–Mars line, Fig. 1.

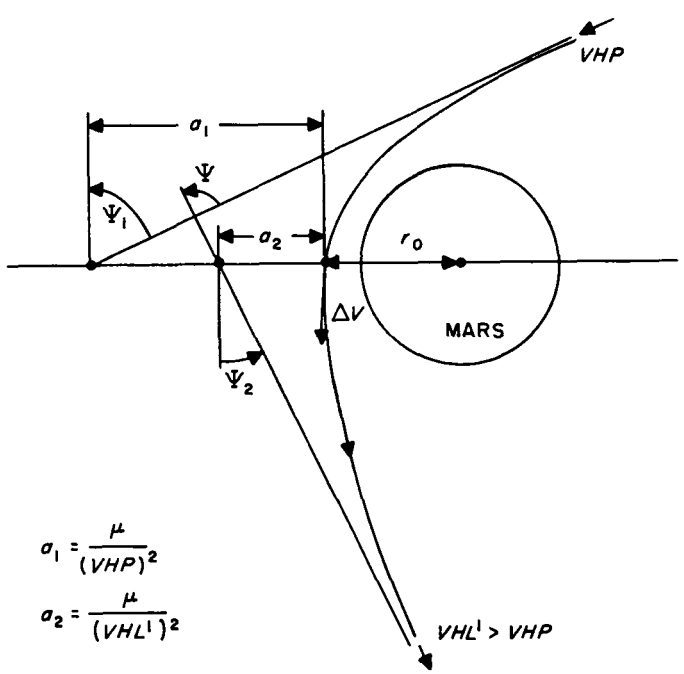

Fig. 1. Lighting conditions for Mars flyby

[2]The principal notation is summarized at the end of this Report.

[3]DVL is easily converted to conventional energy units C_3 or hyperbolic excess velocity at Earth VHL by means of the following equation:

$$C_3 = (VHL)^2 = (7.8 + DVL)^2 - 121.7 \text{ (km/sec)}^2$$

where DVL and VHL are in km/sec.

Given TA, the day of the departure from Mars, and TA', the Mars–Earth return conic is easily found and results in the following trajectory parameters:

VHL' – the asymptotic speed with respect to Mars at the beginning of the return trajectory.

ψ – the angle between the incoming asymptote and the outgoing asymptote at Mars, sometimes called the bending angle.

VHP' – the asymptotic speed at Earth encounter.

$ZALD$ – the angle between the outgoing asymptote at Mars and the Sun–Mars direction, Fig. 1.

If the approach and departure asymptotic velocities at Mars are equal, no velocity increment has to be imparted to the spacecraft near Mars, and the unique flyby altitude above the Mars surface is given by:

$$H_P = \frac{\mu}{VHP^2}\left(\frac{1}{\sin(\psi/2)} - 1\right) - r_0 \qquad (1)$$

If the approach and departure asymptotic velocities at Mars are not equal, a velocity correction in the vicinity of Mars is necessary to achieve the desired Earth-return trajectory. We shall consider encounter trajectories where, at most, one impulsive maneuver is carried out. Table 1 shows the flyby altitudes and required velocity increments for maneuvers carried out at the following three points on the Mars encounter trajectory:

1. A great distance from Mars before encounter.
2. The common periapsis of both encounter hyperbolas.
3. A great distance from Mars after encounter.

For 1 and 3, the maneuvers are colinear. The flyby trajectory consists of a single hyperbola only. For 2, the flyby altitude H_P is specified by the transcendental equation, Fig. 2:

$$\psi = \sin^{-1}\left[1 + \frac{\mu(r_0 + H_P)}{(VHP)^2}\right]^{-1} + \sin^{-1}\left[1 + \frac{\mu(r_0 + H_P)}{(VHL')^2}\right]^{-1} \qquad (2)$$

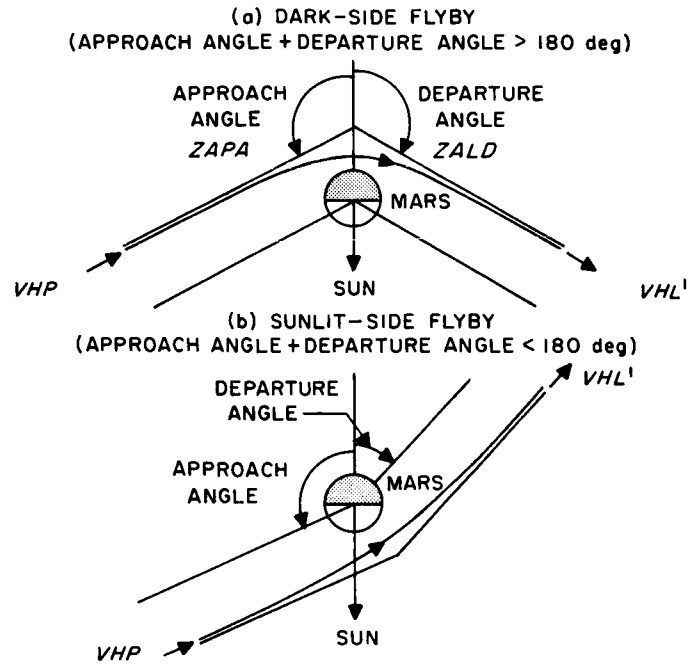

Fig. 2. Mars encounter geometry

and the encounter trajectory consists of two hyperbolic segments patched at periapsis. The velocity increment is:

$$DV = \left(VHP^2 + \frac{2\mu}{r_0 + H_P}\right)^{1/2} - \left(VHL' + \frac{2\mu}{r_0 + H_P}\right)^{1/2} \qquad (3)$$

It is easily shown that:

$$H_{P1} > H_P > H_{P2}$$

$$DV < |VHP - VHL'|$$

if

$$VHP < VHL'$$

In general, it is possible to reduce the velocity increment somewhat below DV (Ref. 4).

Table 1. Flyby altitude and required ΔV for three types of maneuvers

Point of maneuver	η_1	η_2	h_m	h_c	ΔV
A large distance from Mars before encounter	---	$-\left[90 \text{ deg} + \left(\frac{\psi}{2}\right)\right]$	∞	$H_{P2} = \frac{\mu}{(VHL')^2}\left[\csc\left(\frac{\psi}{2}\right) - 1\right] - r_0$	$DVP = \lvert VHP - VHL' \rvert$
Common periapsis of both encounter hyperbolas	0	0	H_P	$H_P(\psi)$ (Eq. 1)	DV (Eq. 3)
A large distance from Mars after encounter	$90 \text{ deg} + \left(\frac{\psi}{2}\right)$	---	∞	$H_{P1} = \frac{\mu}{(VHP)^2}\left[\csc\left(\frac{\psi}{2}\right) - 1\right] - r_0$	$DVP = \lvert VHP - VHL' \rvert$

ψ = bending angle, η_1/η_2 = true anomaly of transfer point on the incoming/outgoing hyperbola.

III. PRESENTATION OF TRAJECTORY DATA

Trajectory data for one-way transfer from the Earth to other planets are most conveniently presented in the form of contour charts, as shown in Fig. 3. This figure shows contours of constant injection ΔV, DVL, for Earth–Mars Type I trajectories to be launched in 1969. The region of *Mariner* Mars 1969 trajectories is indicated in the same figure.

Similar charts have been prepared for Earth–Mars, Earth–Venus, Earth–Mercury and Earth–Jupiter transfer and represent a valuable tool in the design of such trajectories (Ref. 1). It is important to note that each point in Fig. 3 represents exactly one Earth–Mars trajectory.

With the consideration of Earth–Mars–Earth trajectories, a new independent variable—the total trip time T—is introduced. For a given TL and TA, we are not interested in all possible Earth–Mars–Earth trajectories, but only the optimized one which results in:

1. A reasonable value of T, the total trip time.
2. The maximum payload or minimum energy; i.e., the minimum velocity increment DV at Mars.
3. One of the flyby altitudes HP, H_{P1}, H_{P2} being greater than zero.
4. The total ΔV requirement, $DVT = DVL + DV$, not to be excessive.

In this Report, the upper limit on DVT was arbitrarily selected to be $DVTM = 7.1$ km/sec [$C_3 = 100$ (km/sec)^2]. In our optimization, it does not matter how DVT is distributed between DVL (the ΔV at launch) and DV (the ΔV at Mars). Actually, it is much easier to impart a large ΔV at Earth and a small ΔV at Mars, rather than vice versa.

The actual mission payload (exclusive of the propulsion system) will depend not only on DVT but also on the way DVT is distributed between DVL and DV. The DVT can be used as a parameter which specifies payload as a first approximation, just as DVL is used to evaluate mission payload for one-way trajectories.

IV. COMPUTER PROGRAM DESCRIPTION

For each Mars opportunity to be studied, the region in the TL–TA plane, with DVL less than $DVTM$, is found from available Earth–Mars trajectory data. The minimum and maximum values of T, T_{MIN}, and T_{MAX} must be specified, as well as the minimum altitude at Mars H_{MIN}. In this study, we use $T_{MIN} = 350$ days, $T_{MAX} = 650$ days, and $H_{MIN} = 0$.

The program then computes all the Earth–Mars–Earth trajectories beginning with the lowest value of TL and the highest of TA. TL is first increased over the range of TLs, and TA is then decreased. For each TL and TA, T is varied between T_{MIN} and T_{MAX} with a certain increment DTF. If the launch energy and flyby altitude constraints are met, the trajectory parameters are computed and printed; otherwise the trajectory is rejected. Simultaneously, for each TL and TA, a buffer is provided which, at any time, contains the trajectory data corresponding to the minimum DVP trajectory. Of course, the purely ballistic trajectory which corresponds to $DVP = 0$ is the most interesting one. Consequently, if the program detects a change in sign in DVP, a linear interpolation in T is performed, and the corresponding trajectory data are computed and are then stored in the buffer. The program then continues with the computation of all Earth–Mars–Earth trajectories until $T = T_{MAX}$.

After all desired Earth–Mars–Earth trajectories have been computed, the program prints out a convenient trajectory matrix containing 13 important trajectory parameters contained in the buffer, corresponding to the optimized (minimum DVP) Earth–Mars–Earth trajectories. In this matrix, the abscissa is TL, and the ordinate is TA. These data are then used to generate the contour charts used in the trajectory design. Machine plotting routines are available.

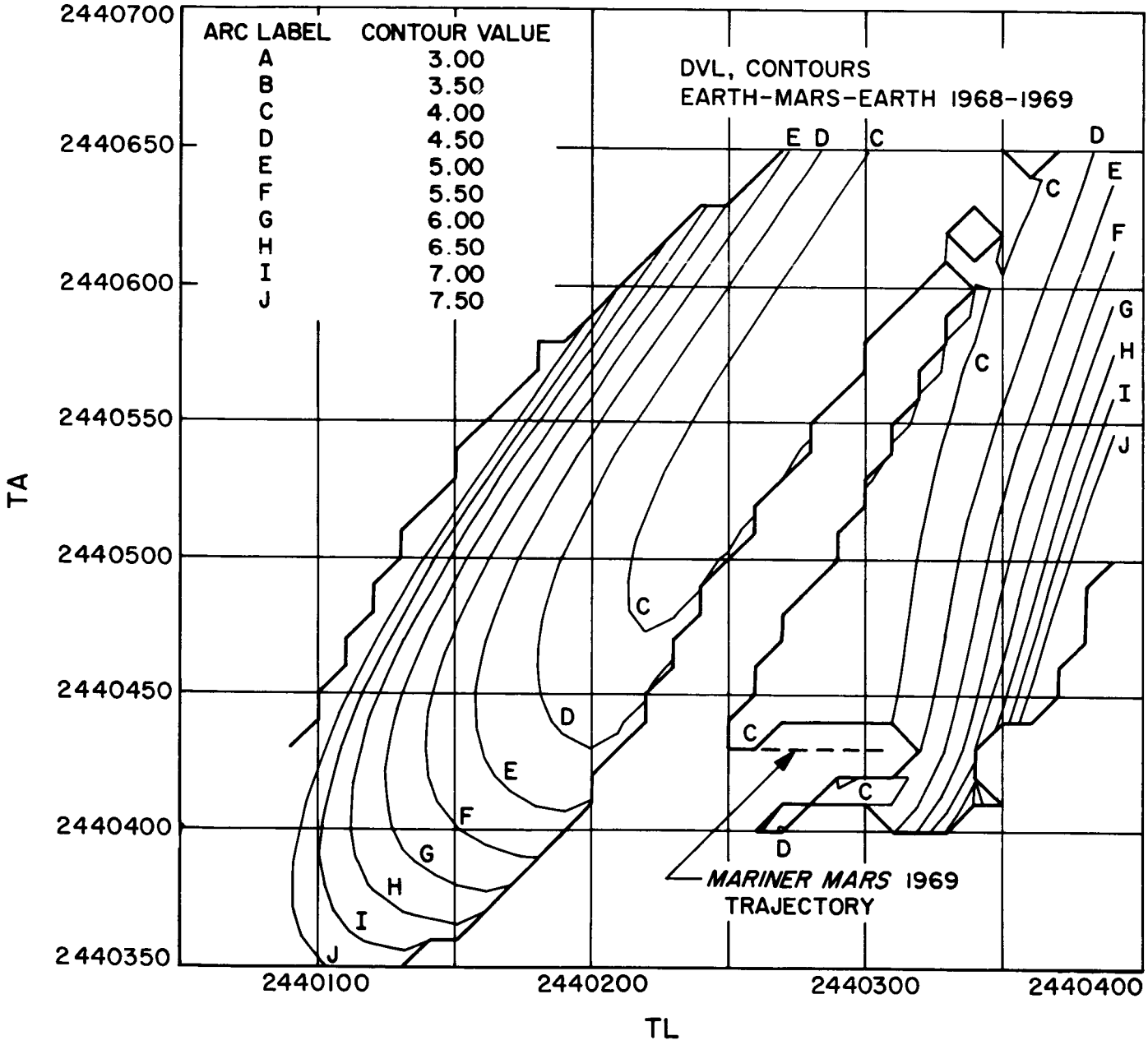

Fig. 3. *DVL* contours. Earth–Mars–Earth 1968–1969

V. DISCUSSION OF CONTOUR PLOTS

Figures 3–16 are the contour charts of the trajectory parameters used to design the Earth–Mars–Earth trajectories for launch in 1969 and 1971. Figures 3 and 10 show the total ΔV requirement for these missions in 1969 and 1971, respectively. Figures 4 and 11 show the parameter *DVP* for both opportunities. In Figs. 4 and 11, the regions corresponding to $DVP = 0$ are indicated. Within these regions, the Earth–Mars–Earth trajectories are purely ballistic after injection near the Earth. If the contour charts are compiled in the form of convenient transparent overlays, it is possible to read off several trajectory parameters at the same time. For example, by overlaying Figs. 3 and 4, one finds the ΔV requirement for the purely ballistic Earth–Mars–Earth trajectories. It can be seen that for the 1969 opportunity, the regions of zero *DVP* are somewhat removed from the regions of minimum *DVL*. The *DVT* is the total velocity increment required for the mission. It will be seen that, in 1971, these regions are closer together, which results in much more favorable Earth–Mars–Earth trajectories. Figures 6 and 13 show contours of flyby altitude at Mars if a periapsis maneuver is performed.

The parameter *ZAPA* gives approximate approach conditions at Mars (Fig. 2). If *ZAPA* is smaller than 90 deg, the sub-vehicle point on approaching the planet lies over a dark region; if it is greater than 90 deg, the sub-vehicle point lies over a sunlit region. Similarly, the departure angle *ZALD* is an indication of lighting conditions when leaving Mars. Depending on whether *ZALD* is smaller or greater than 90 deg, the sub-vehicle point at departure lies above a dark or sunlit region of Mars.

Lighting conditions during Mars encounter are indicated by the sum of the approach angle *ZAPA* and the departure angle *ZALD*. If the sum, *ZAPA* + *ZALD*, is greater than 180 deg, the vehicle periapsis point lies above the dark region of Mars (Fig. 2). If the sum, *ZAPA* + *ZALD*, is smaller than 180 deg, the periapsis point lies above a sunlit region at Mars. We thus refer to *dark side flyby* and *sunny side flyby*. Regions of dark side and sunny side flybys at Mars are also indicated in Figs. 5 and 12.

The one-way Earth–Mars trip time contours, which consist of straight lines running from the upper right to the lower left of the diagrams, have not been indicated here. Finally, the trajectory parameter *T*, the total trip time, is of interest.

VI. 1971 OPPORTUNITY

Figures 10–16 show the contour plots of the trajectory parameters for the 1971 opportunity. A comparison of Figs. 10 and 11 shows that there is a larger region corresponding to $DVP = 0$, and that, within this region, there is a large number of trajectories with *DVP* on the order of 6 km/sec. The region also includes primarily sunny side flybys, of greater interest for photography missions. Total mission times extend from 500 to 550 days. Flyby altitudes are on the order of one Martian radius.

Higher payloads and shorter missions can be achieved with the use of dark side flybys. However, in this case, substantial velocity increments at Mars are required. For example, for $TL = 2441080$, $TA = 2441250$, the ΔV at launch is $DVL = 5.1$ km/sec, and the velocity increment is 2.1 km/sec. The velocity increment is imparted after Mars encounter and the flyby distance is 448 km. The total trip time is 420 days while the Earth-to-Mars flight time is 170 days.

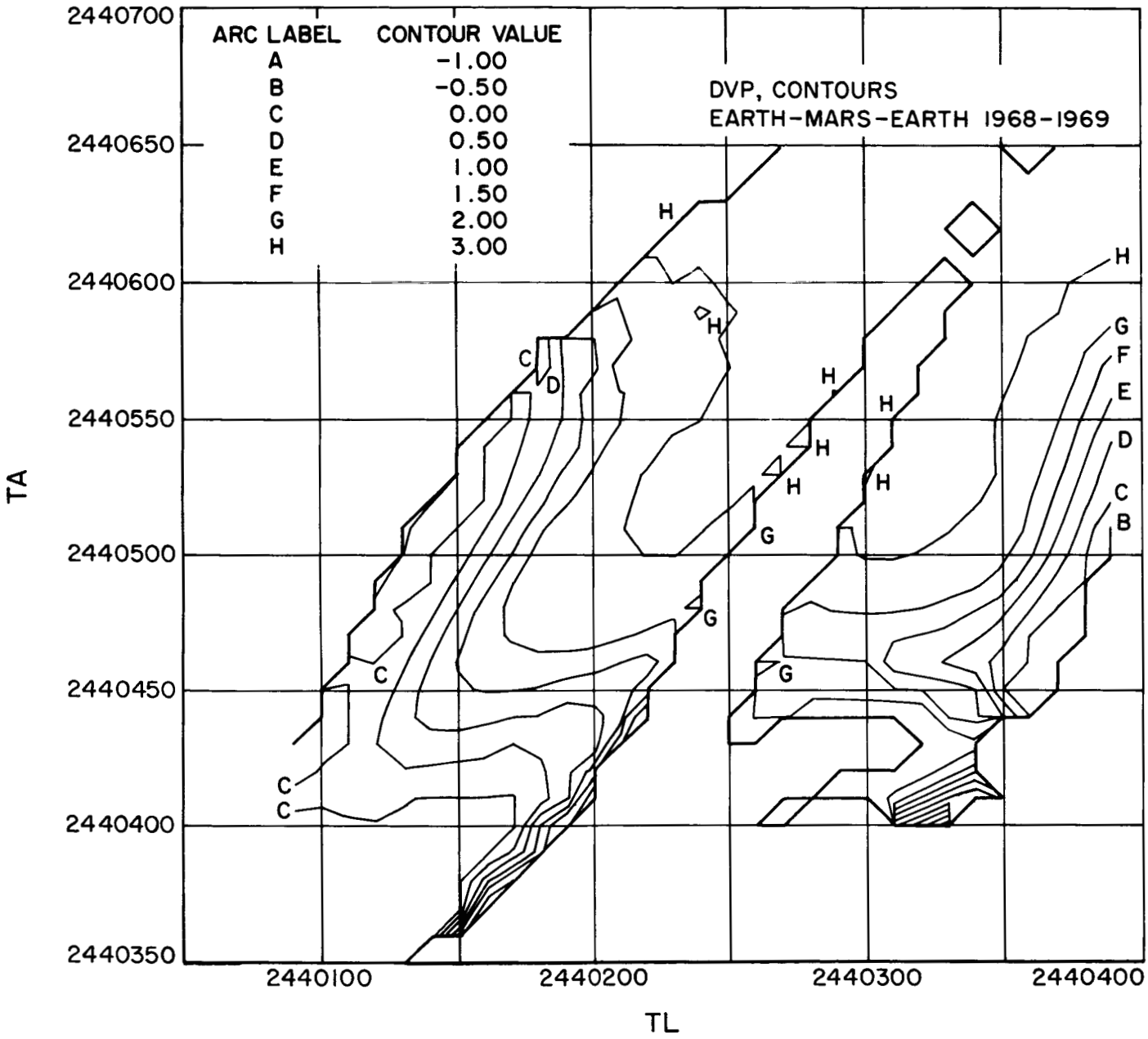

Fig. 4. *DVP* contours. Earth–Mars–Earth 1968–1969

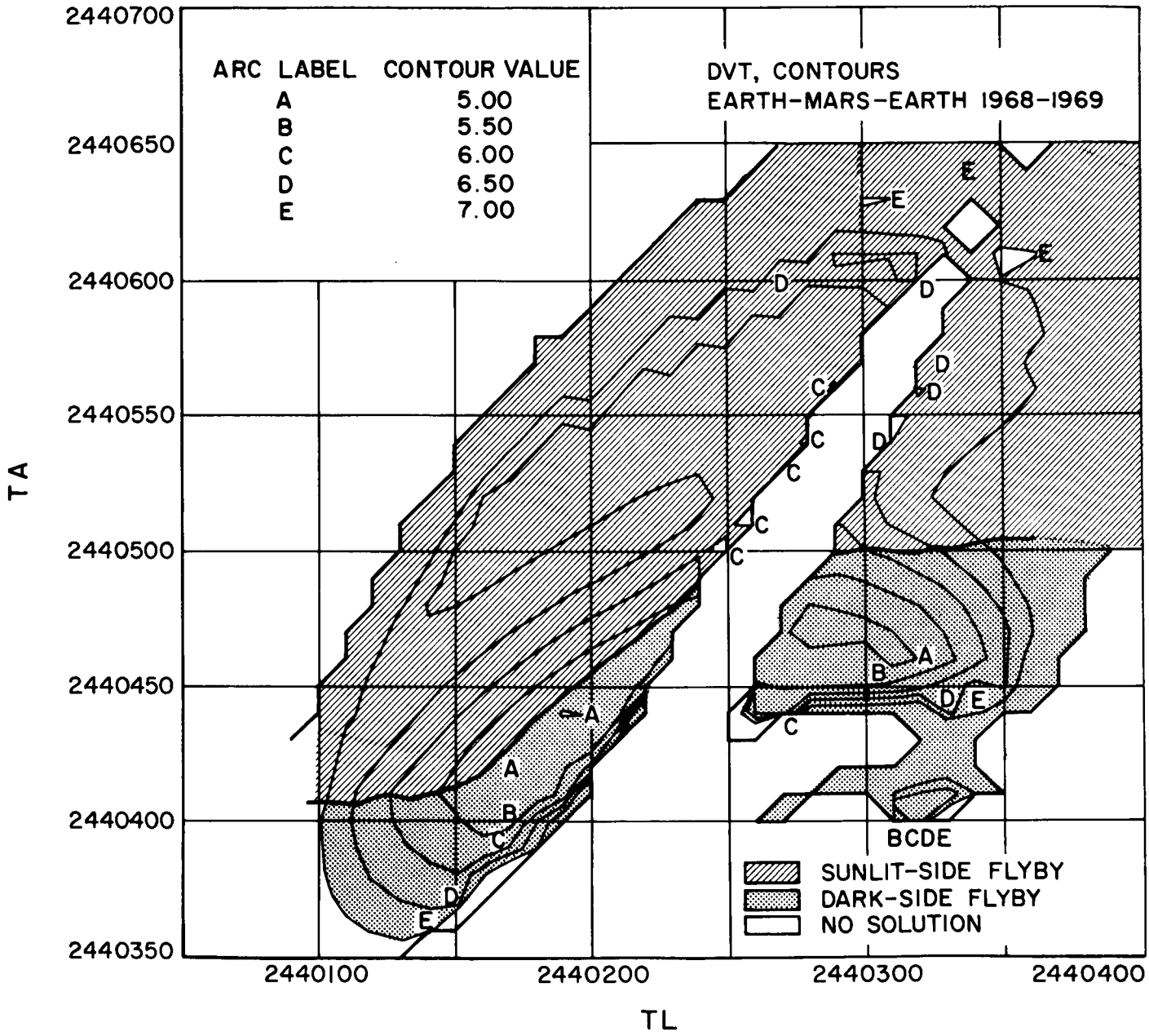

Fig. 5. *DVT* contours. Earth–Mars–Earth 1968–1969

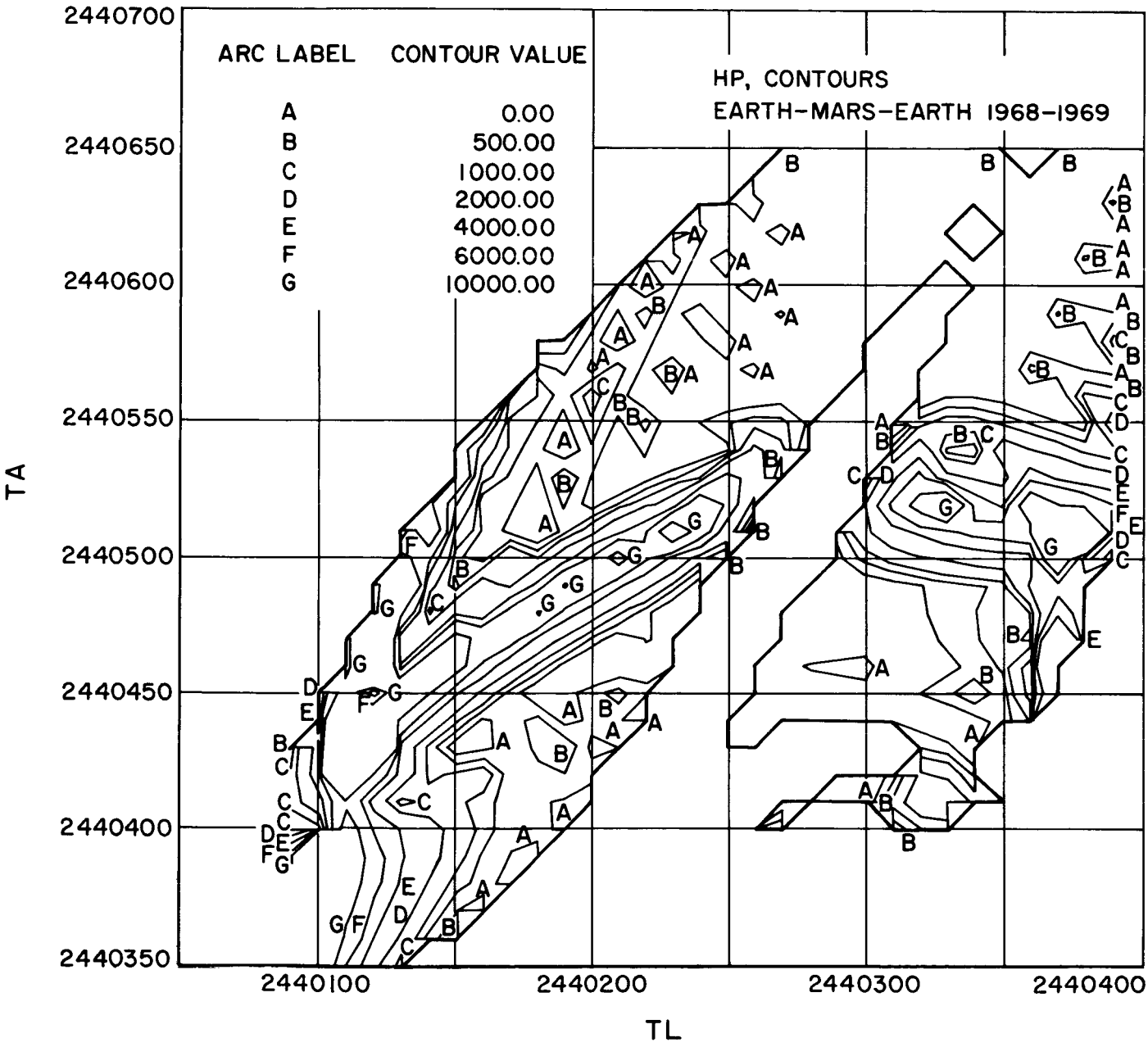

Fig. 6. *HP* contours. Earth–Mars–Earth 1968–1969

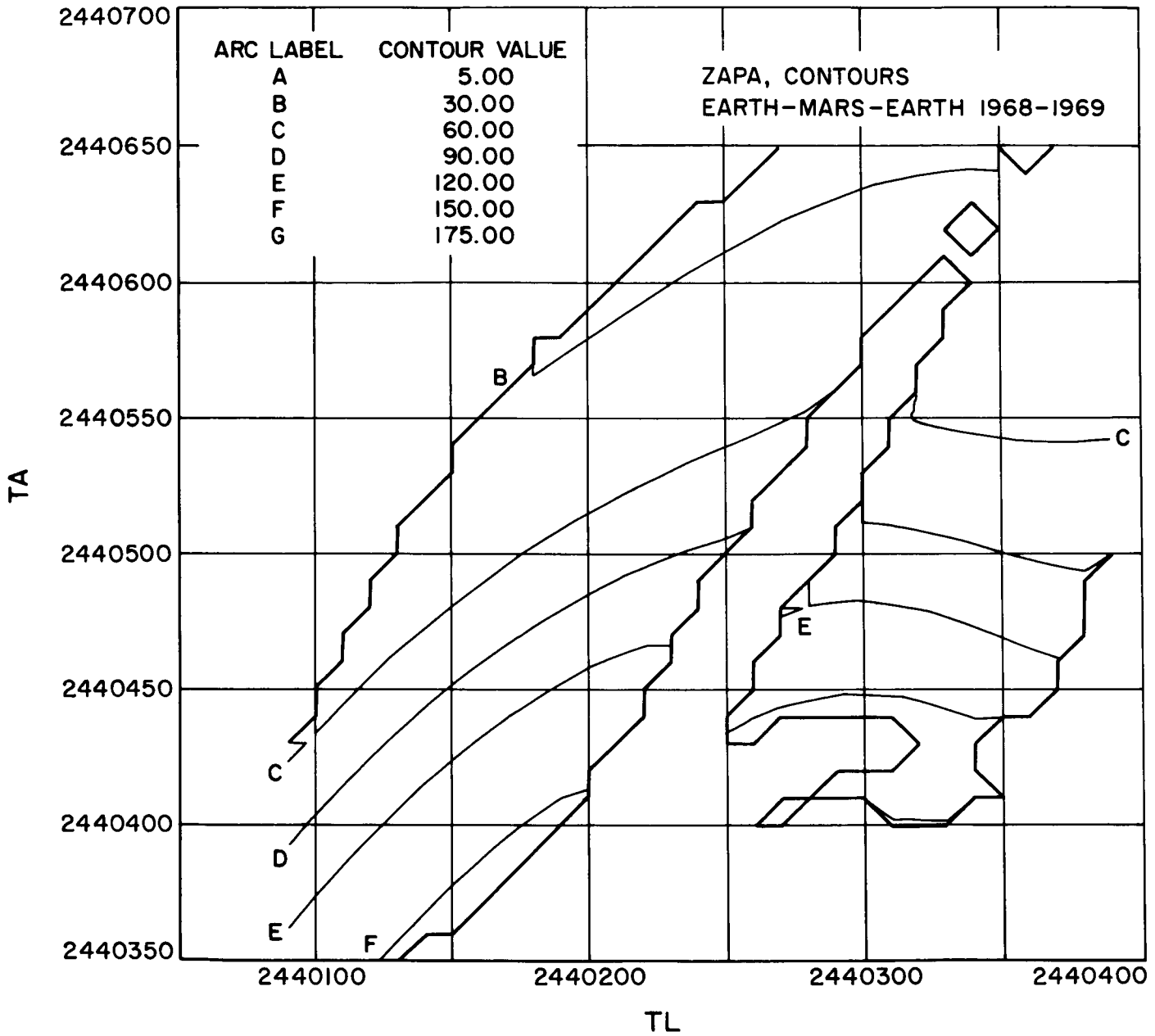

Fig. 7. *ZAPA* contours. Earth–Mars–Earth 1968–1969

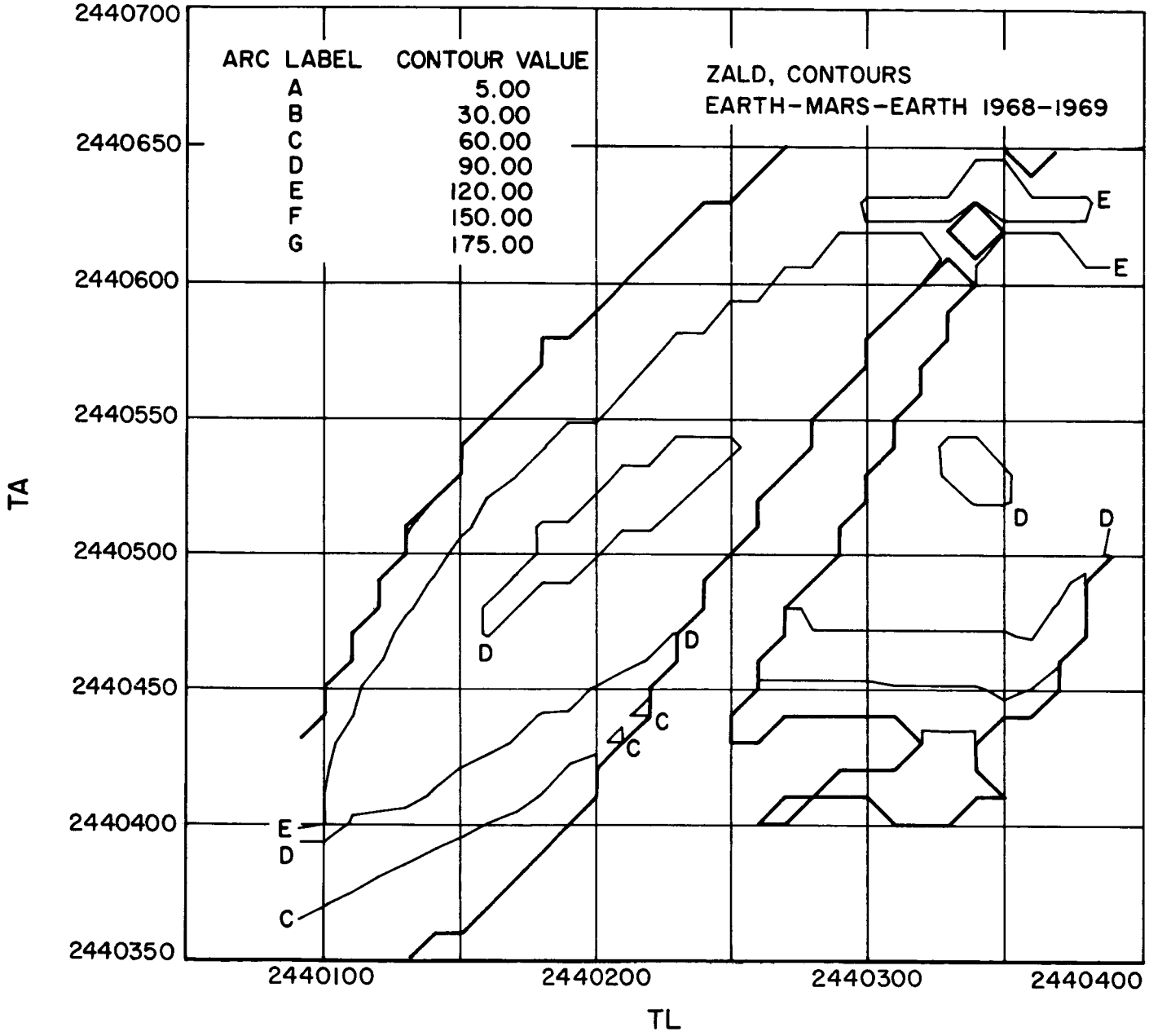

Fig. 8. *ZALD* contours. Earth–Mars–Earth 1968–1969

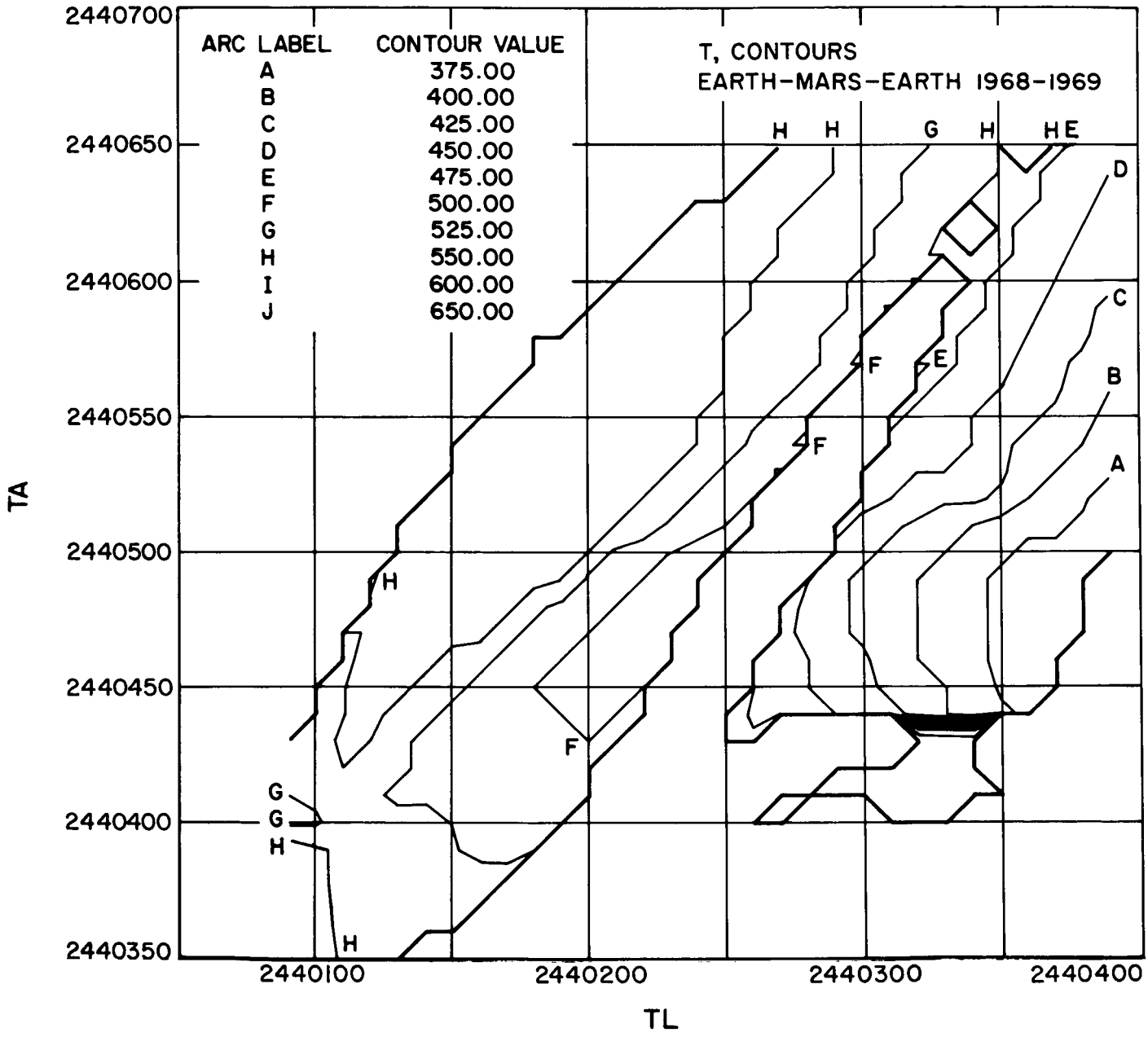

Fig. 9. *T* contours. Earth–Mars–Earth 1968–1969

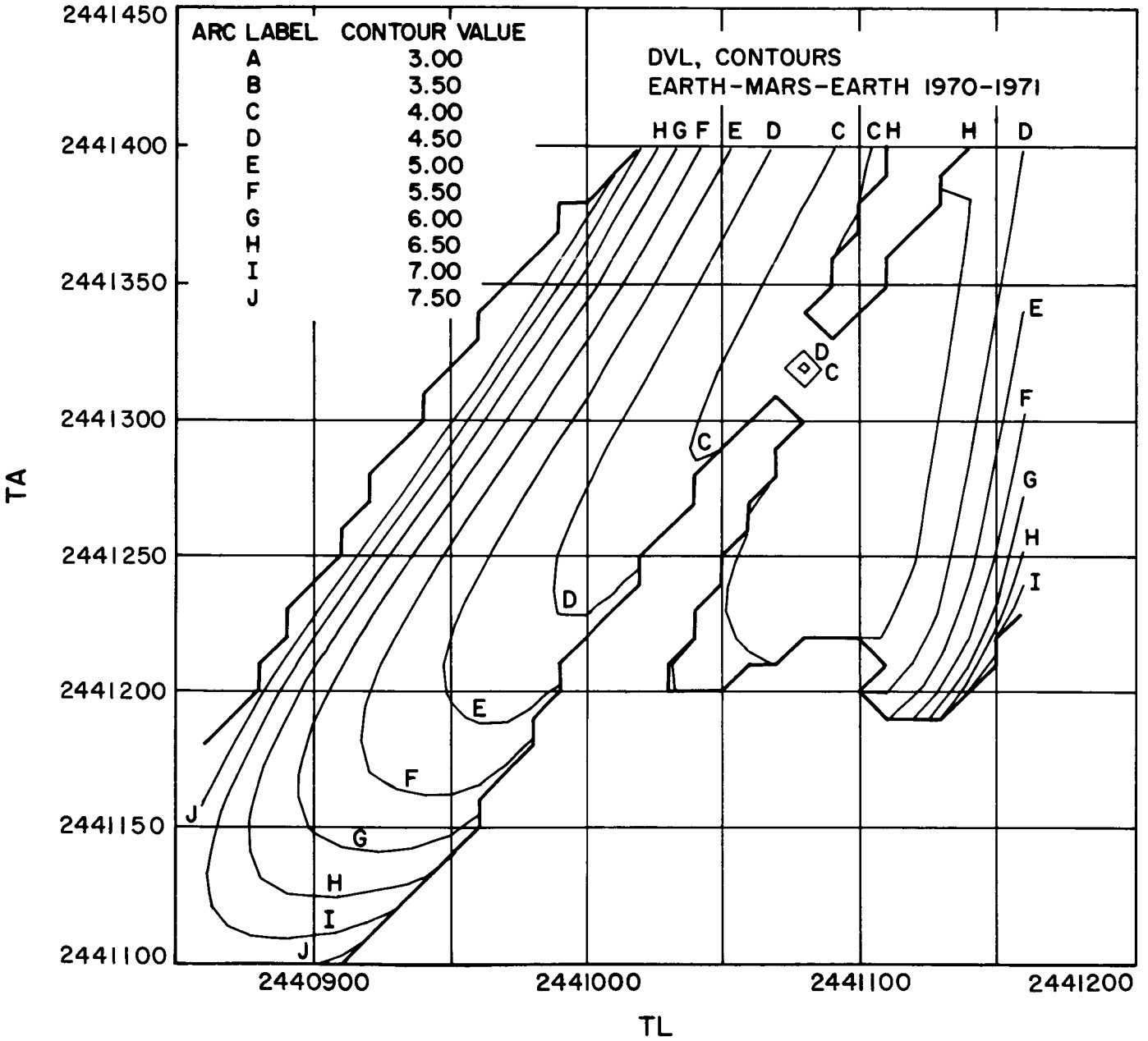

Fig. 10. *DVL* contours. Earth–Mars–Earth 1970–1971

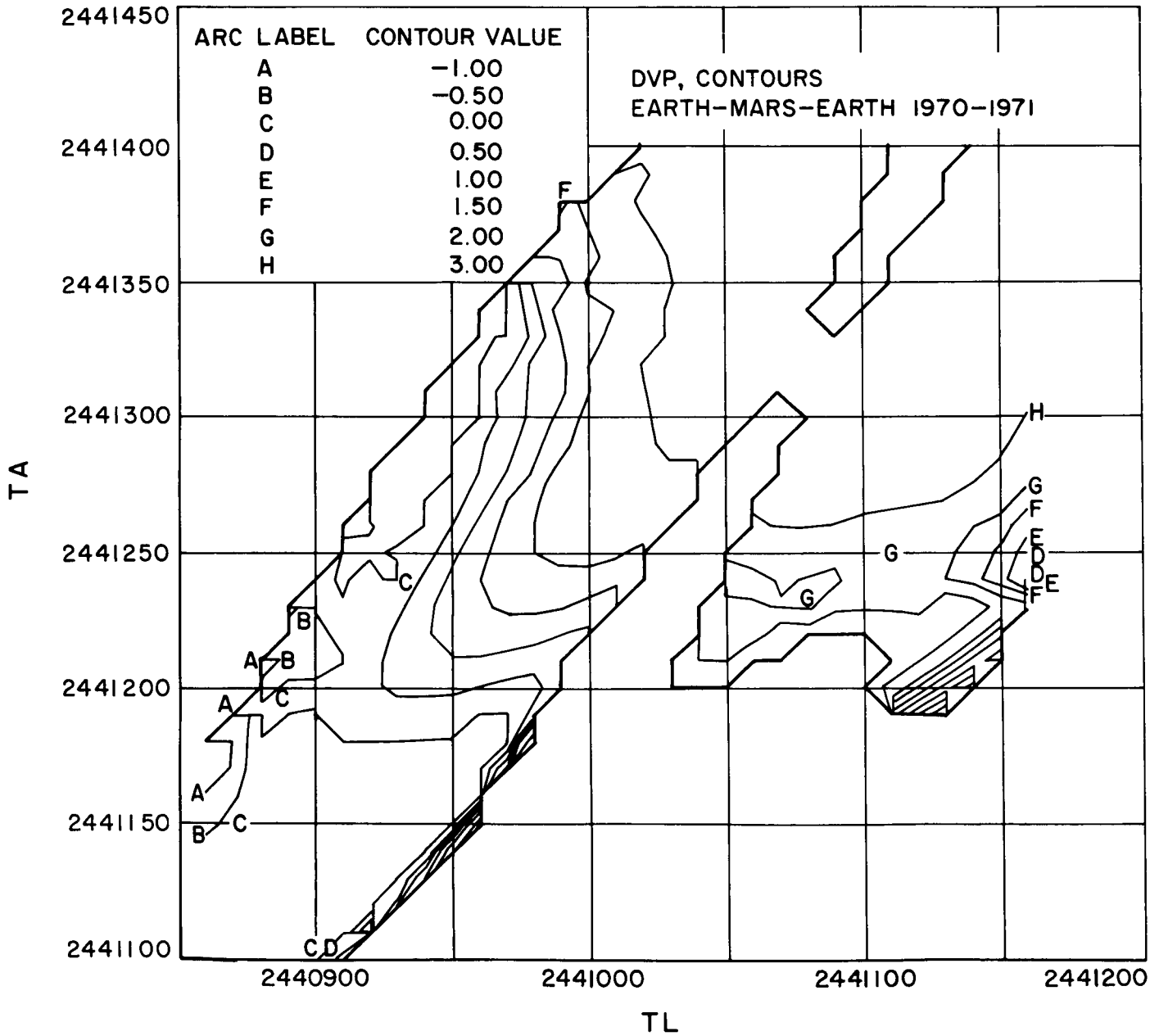

Fig. 11. *DVP* contours. Earth–Mars–Earth 1970–1971

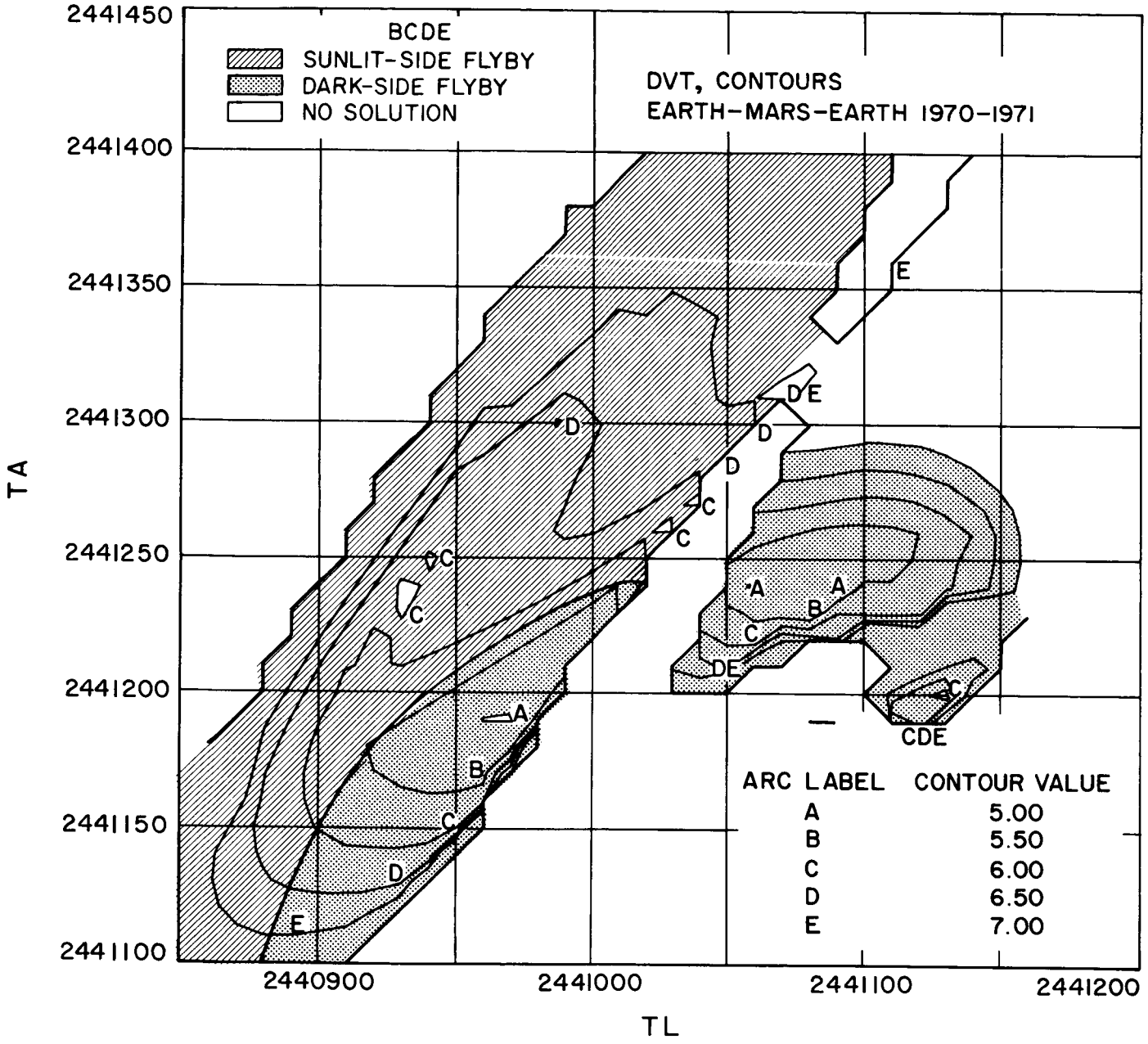

Fig. 12. *DVT* contours. Earth–Mars–Earth 1970–1971

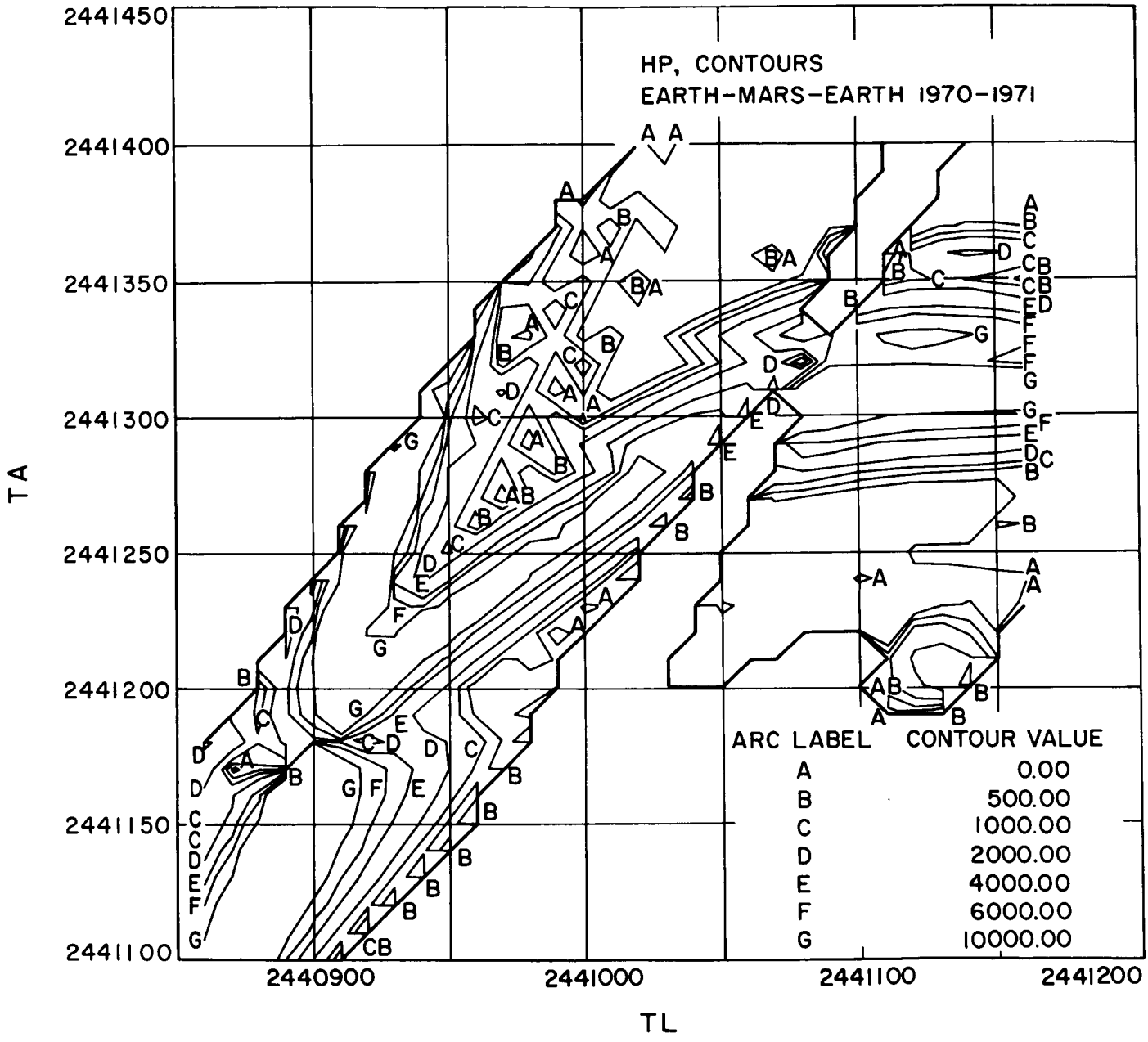

Fig. 13. *HP* contours. Earth–Mars–Earth 1970–1971

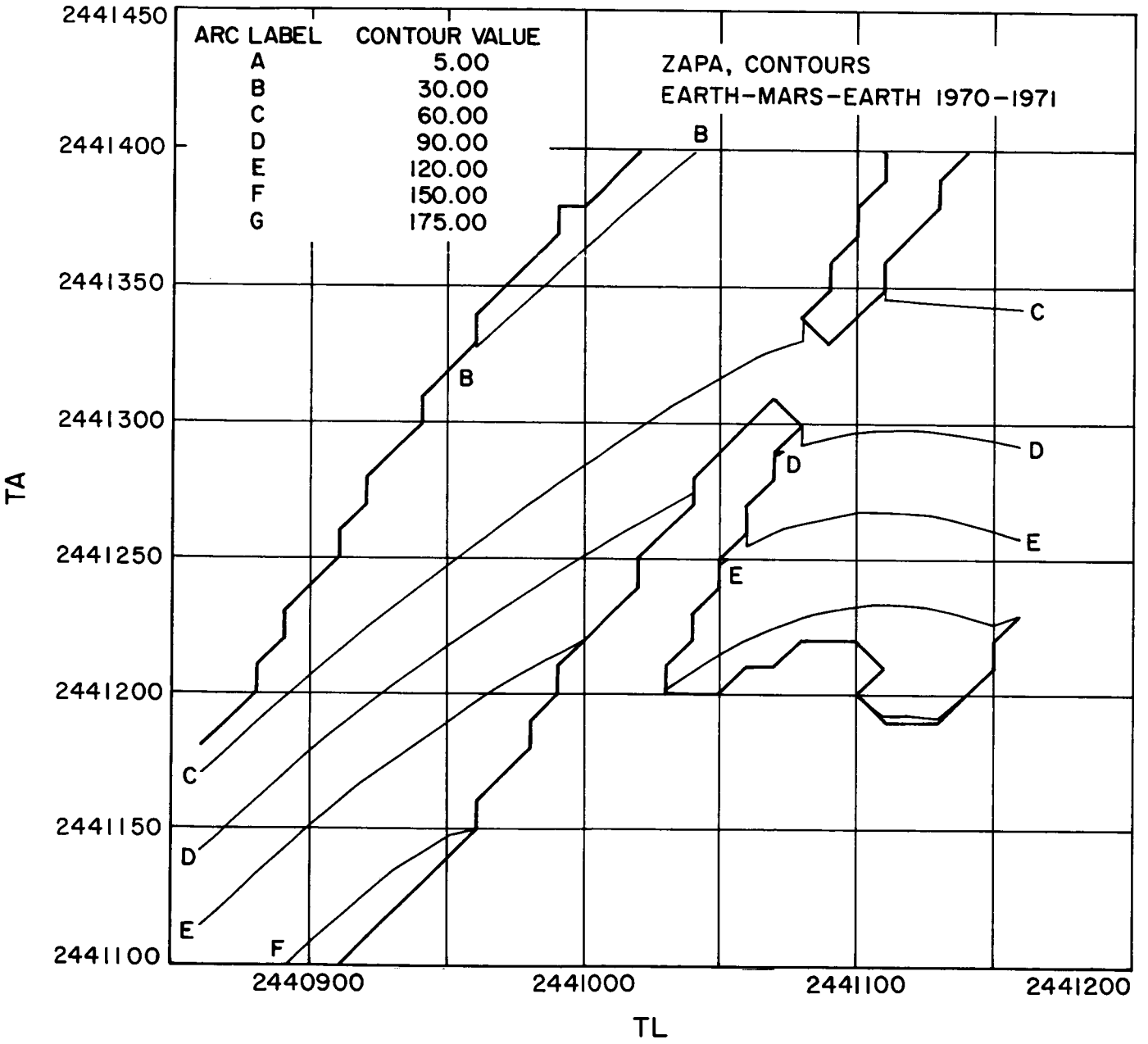

Fig. 14. *ZAPA* contours. Earth–Mars–Earth 1970–1971

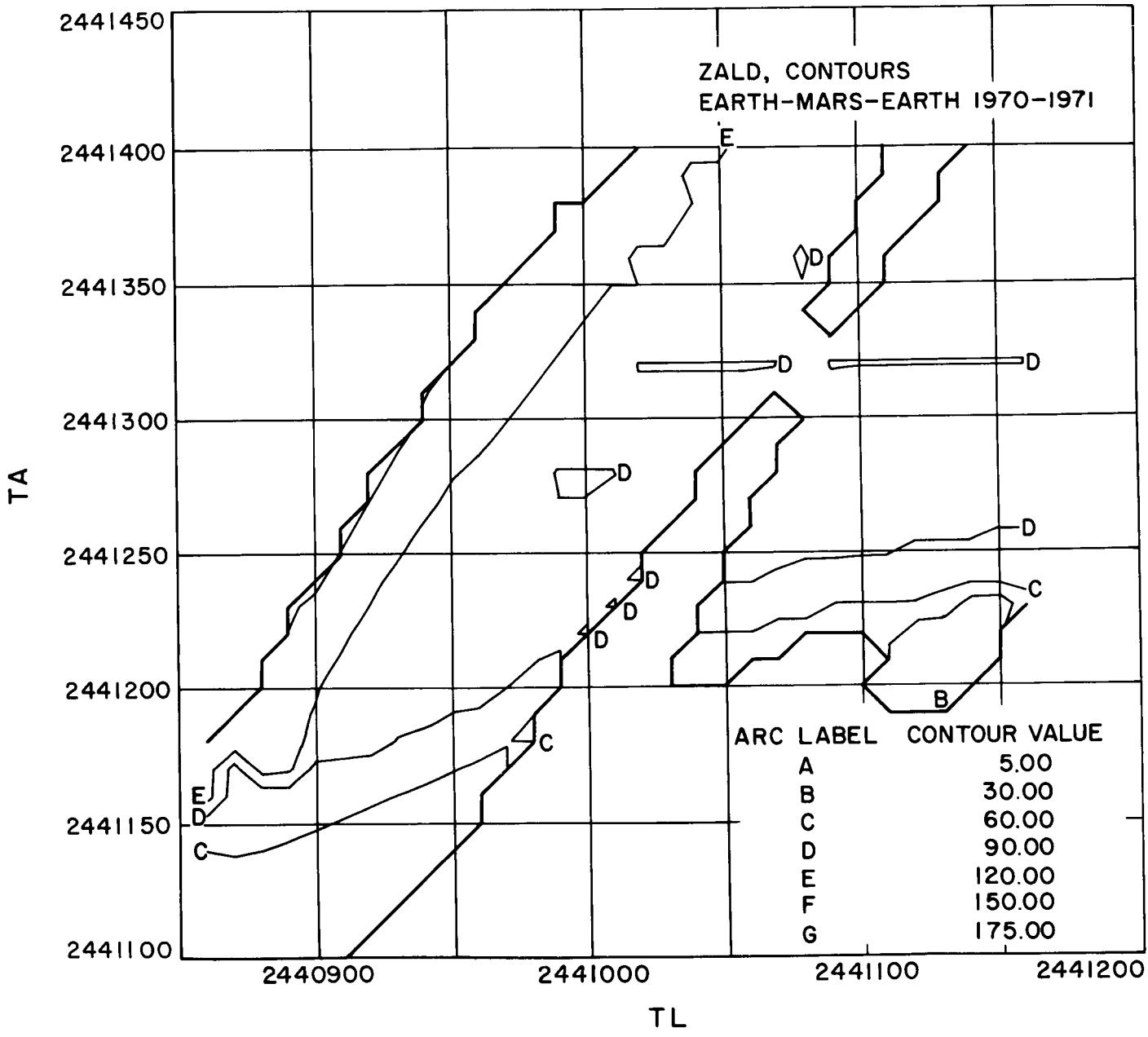

Fig. 15. *ZALD* contours. Earth–Mars–Earth 1970–1971

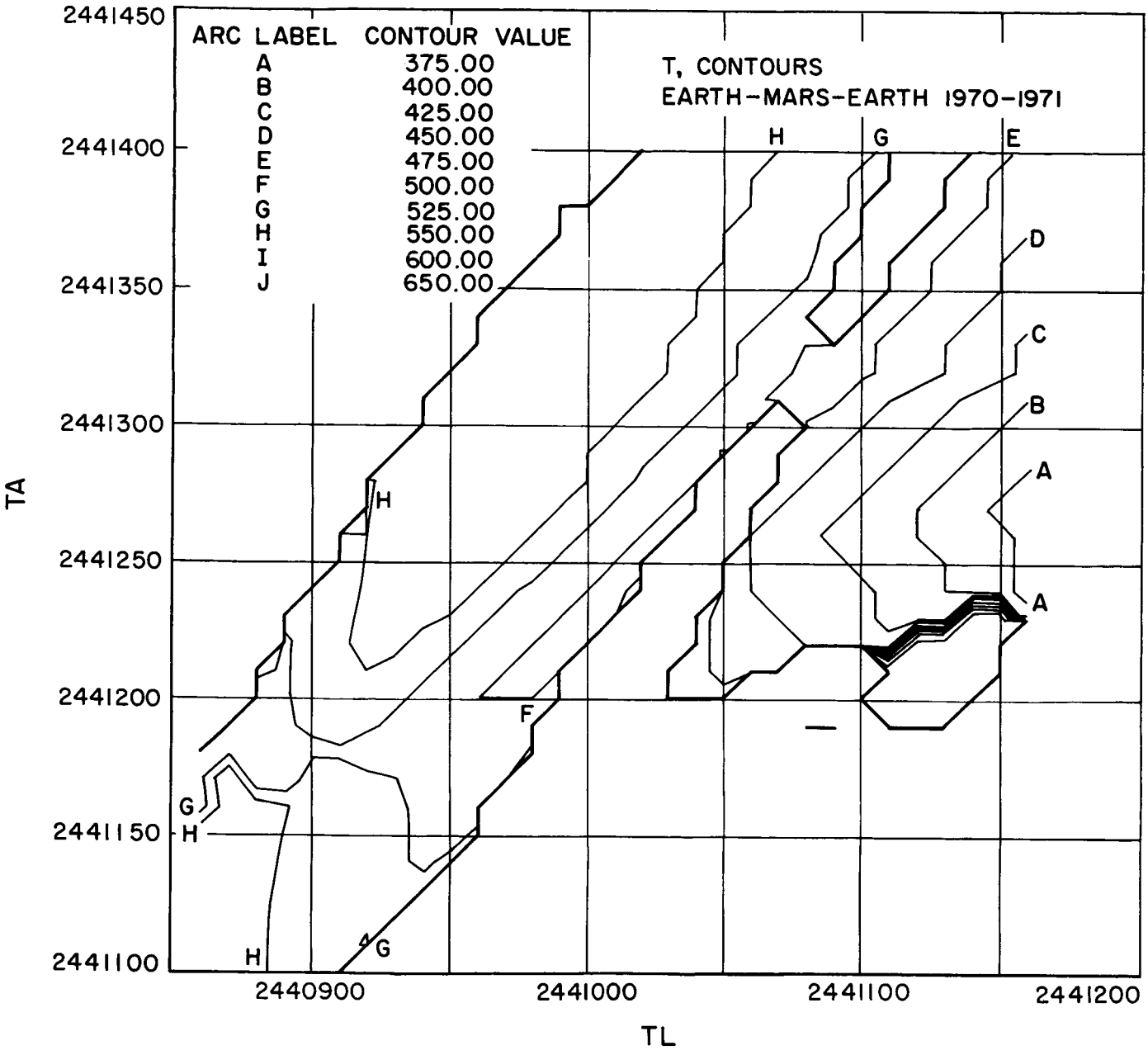

Fig. 16. *T* contours. Earth–Mars–Earth 1970–1971

VII. COMMUNICATION ADVANTAGE OF AN EARTH–MARS–EARTH MISSION

After *Mariner IV* encountered Mars in 1965, about five million bits of Mars encounter data comprising 22 photographs were transmitted back to Earth over a period of 7 days. The data rate was 8⅓ bps during this period.

For example, we shall show the communication advantage of a typical Earth–Mars–Earth trajectory launch in 1971. The Earth departure date is 2440936, the Mars arrival date is 2441248, and the total trip time is 574 days. The Mars-to-Earth flight time is 262 days. The projection of the Mars-to-Earth trajectory onto the heliocentric plane is shown in Fig. 17. The probe departs from Mars on October 21, 1971, at which time the Earth-probe range is increasing. The maximum communications distance is reached on $t = 120$ days from Mars departure. From this point on, the communication distance decreases up to Earth encounter, which occurs at $t = 262$ days.

In the following, we shall draw a comparison with a Mars orbiter which is assumed to begin transmission on October 24, 1971. For the orbiter, the communication distance is an increasing function of time up to $t = 262$ days.

It will be assumed that the orbiter and the Earth return probe both begin transmission on October 24, 1971, at a data rate of 50 bps. For both vehicles, the data rate is decreased or increased by factors of 2 whenever possible, according to communication distance to the Earth. For the orbiter, the data rate must be decreased three times over the 262 days. Based on communication distance alone, the data rate of the Earth return probe would have to be decreased once and increased 21 times over the 262 days. This would result in a theoretical maximum data rate at Earth encounter of 50×10^6 bps, which is beyond the present state of the art.

Figure 18 shows the total information received over the 262 days for the Earth return probe and the Mars orbiter. The information returned was also computed, assuming the maximum possible data rates were approximately equal to 10^5, 10^6, and 10^7 bps. Due to our assumptions, the actual data rates over the missions will be multiples of 50 bps.

At the end of 40 days, the Earth return probe and the Mars orbiter will have transmitted 1.73×10^8 bits and 1.65×10^8 bits, respectively. At $t = 258.8$ days, the data rate is increased to 102,400 bps. At $t = 259.6$ days, the communication distance has decreased sufficiently so that the data rate could again be doubled. If the data rate is doubled, the information received follows the upper curve. If it is assumed that the maximum data rate is $\dot{I}_m = 102{,}400$ bps, the information received during the Earth encounter phase is shown by the lower curve labeled $\dot{I}_m = 102{,}400$ bps. Such a probe would continue transmitting at this data rate during the entire period of Earth encounter. At the time of Earth encounter ($t = 262$ days), the return probe would have transmitted 495×10^8 bits. Because of symmetry, the communication distance would not become too large for this data rate until $t = 264.4$ days, or 2.4 days after Earth encounter. At this time, the total information received would be 708×10^8 bits, or about 200 times the amount of data sent back by the orbiter. If the maximum data rate were $\dot{I}_m = 819{,}200$ bps, the total information received by Earth-encounter time would be 1432×10^8 bits, and at the time of saturation, the total data received would be 2069×10^8 bits. If the maximum data rate were $\dot{I}_m = 13.1 \times 10^6$ bps, the total data received by Earth-encounter time would be 5748×10^8 bps, and 8012×10^8 bits at $t = 262.2$ days. This latter figure is 2000 times the amount of data returned by the orbiter over the 262 days.

The above figures for information returned assumed that the flyby distance at Earth was 10^5 km, assuming a 1-km circularly distributed error in the **B**-plane at Mars arrival. The **B**-plane is the plane perpendicular to the incoming asymptote at Mars which contains the center of Mars. The ranges of data-range saturation for 102,400 bps, 819,200 bps and 13,107,200 bps are 2.24×10^6 km, 0.78×10^6 km and 195,000 km, respectively. If the flyby distance at Earth is reduced below any of these values, the corresponding information curves shown in Fig. 18 no longer apply. It is only possible to obtain the information shown in Fig. 18 provided that the targeting distance at Earth is less than the saturation distances.

If the targeting distance at Earth were as high as 10^7 km, data rate saturation would take place 10 days before Earth encounter, and the probe would have to transmit at 6400 bps during the 20-day Earth encounter phase. The Earth return probe would thus lose its basic asset, and the data collected would be only an order of magnitude greater than that collected by the orbiter.

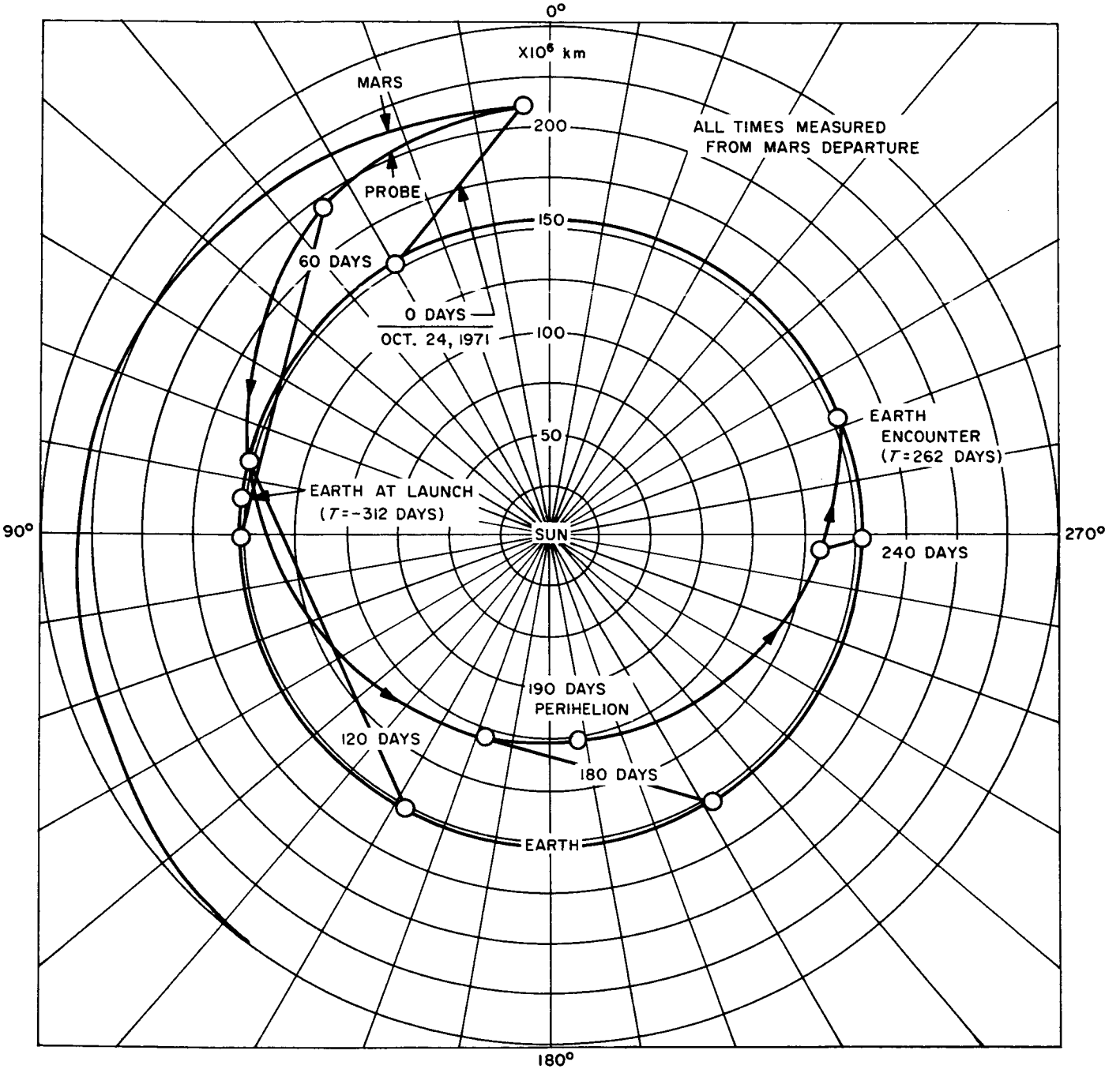

Fig. 17. Ecliptic view of 1971 Earth–Mars–Earth trajectory

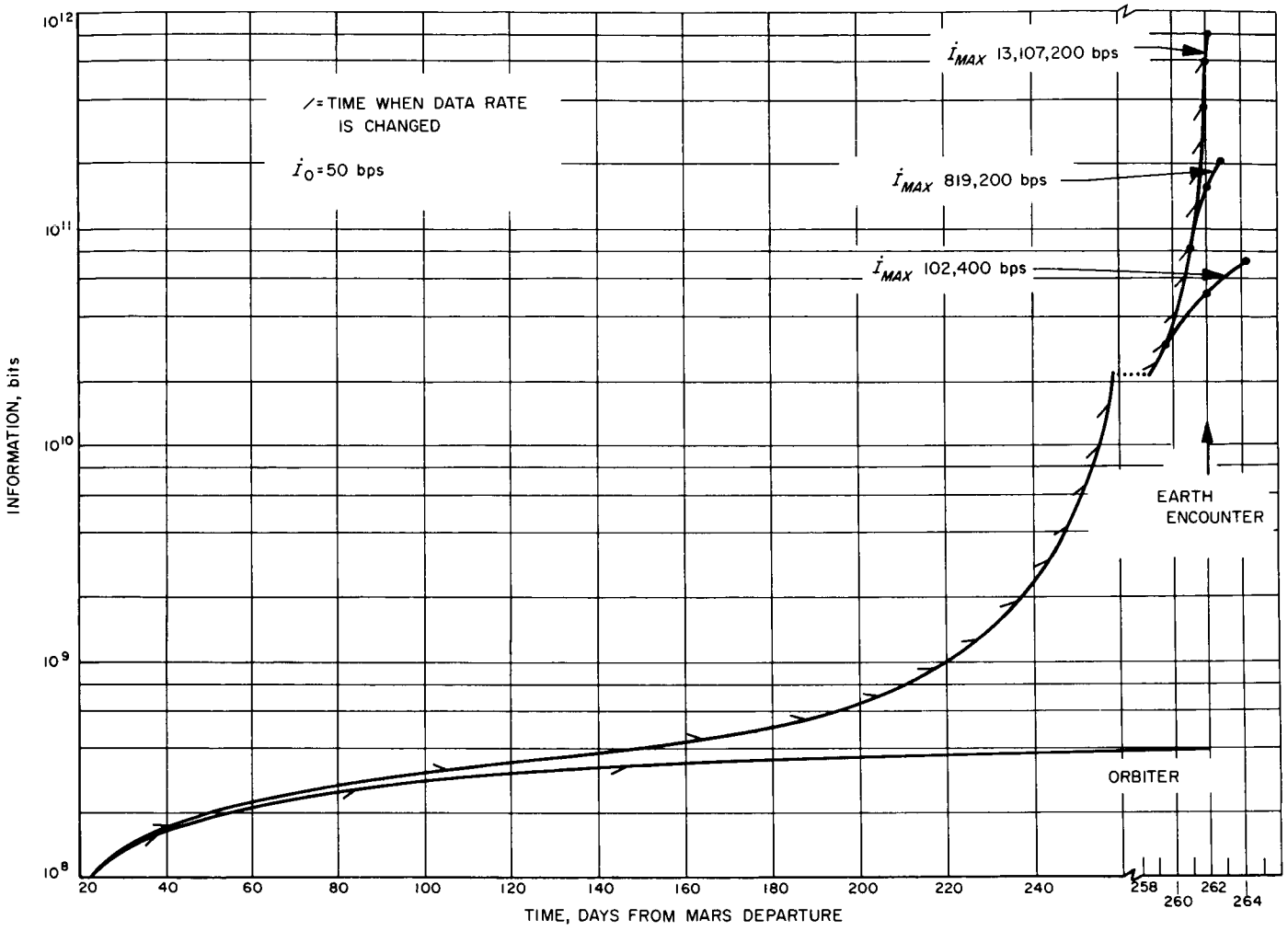

Fig. 18. Time, days from Mars departure

The Earth return probe appears in an even more favorable light if we make the realistic assumption that the Deep Space Instrumentation Facility (DSIF) receiving net could not support a mission which required the collection of data for over ½ yr. For example, suppose the DSIF could be committed for 1 mo of continuous data collection. According to Fig. 18, it would then receive 1.3×10^8 bits of information from the orbiter during this period. Assuming the targeting distance at Earth to be 10^5 km, Fig. 18 shows that the return probe could transmit 416×10^8 bits during the 4.8 days extending from $t = 259.6$ to 264.4 days, transmitting at a constant data rate of 102,400 bps. If the data rate were 819,200 bps, the data collected over 1.8 days during Earth encounter is 1.3×10^{11} bps, or 1000 times the amount of data collected by the orbiter. Finally, if the data rate were 13.1×10^6 bps, the data collected over only 0.4 days during Earth encounter would be 4.4×10^{11} bps, or 3000 times the amount of data collected from the orbiter in 1 mo. Figure 18 shows that by beginning transmission even earlier, it is possible to greatly increase the amount of data collected.

VIII. FLYBY GEOMETRY

The flyby geometry for the 1971 Earth–Mars–Earth trajectory discussed in the previous section is favorable for an Earth occultation experiment. The sub-vehicle point passes into the sunlit region of Mars, and at the time of closest approach—where the altitude of Mars is 1000 km—the field of view is 40 deg and contains the sub-solar point. During most of the encounter trajectory, the sub-vehicle point remains Sun-illuminated and is very close to the Martian equator.

NOMENCLATURE

C_3 Geocentric energy at launch from Earth, in km/sec^2

DLA Declination of the outgoing asymptote at Earth, in deg

DV Velocity increment if maneuver is carried out at Mars periapsis, in km/sec

DVL Velocity increment at Earth from parking orbit, in km/sec

DVP Difference in asymptotic speeds at arrival and departure with respect to Mars, in km/sec

DVT $DVL + DV$; total velocity increment requirement for *impulsive* Earth–Mars–Earth trajectory if maneuver is carried out at Mars periapsis, in km/sec

h_m Altitude above Mars when maneuver is performed, in km/sec

h_c Flyby distance at Mars, in km

H_P Flyby distance at Mars if maneuver is performed at Mars periapsis, in km

H_{P1} Flyby distance at Mars if maneuver is carried out a large distance from Mars before Mars encounter, in km

H_{P2} As above, except after Mars encounter, in km

r_0 3310 km, radius of Mars

T Total mission time for Earth–Mars–Earth trajectory, in days

t Time from Mars departure, in days

TA Julian date of arrival at Mars

TA' Julian date of arrival at Earth

TF Earth–Mars flight time, in days

TL Julian date of launch from Earth

VHL Hyperbolic excess velocity at Earth departure, in km/sec

VHL' Hyperbolic excess velocity at Mars at Mars departure, in km/sec

VHP Hyperbolic excess velocity at Mars at Mars arrival, in km/sec

VHP' Hyperbolic excess velocity at Earth at Earth arrival, in km/sec

$ZALD$ Mars departure angle or angle between the outgoing asymptote at Mars and the Sun–Mars line, in deg

$ZAPA$ Mars arrival angle or angle between the incoming asymptote at Mars and the Sun–Mars line, in deg

ψ Bending angle at Mars or angle between the incoming and outgoing asymptotes at Mars, in deg

μ 42906 km^3/sec^2; gravitational constant of Mars, in km^3/sec^2

ΔV Velocity increment, in km/sec

REFERENCES

1. Clarke, V. C., Jr., et al., *Design Parameters for Ballistic Interplanetary Trajectories, Part I. One-Way Transfers to Mars and Venus. Part II. One-Way Transfers to Mercury and Jupiter*, Technical Report 32-77, Jet Propulsion Laboratory, Pasadena, California, January 16, 1963, and January 15, 1966.

2. Ross, S. E., "Trajectory Design for Planetary Mission Analysis," paper presented at AAS/AAAS Special Astronautics Symposium, San Francisco, California, December 29, 1965.

3. Ross, S. E., *Space Flight Handbooks*, Vol. 3: *Planetary Flight Handbook*, NASA SP-35, Part I, National Aeronautics and Space Administration, Washington, D. C., August 1963.

4. Gobetz, F. W., "Optimum Transfers Between Hyperbolic Asymptotes," *AIAA Journal*, Vol. 1, No. 9, Sept. 1963.

ACKNOWLEDGMENT

The author gratefully acknowledges the valuable assistance contributed by Donald C. Snyder who designed the computer program and associated machine plotting routines. The author is also indebted to Dr. P. K. Eckman, J. Billy, and F. Sturms for their contribution to the work presented in this Report.